

Ruthenium counterstaining for imaging mass cytometry

Raúl Catena¹ , Luis M Montuenga² and Bernd Bodenmiller^{1*}

¹ Institute of Molecular Life Sciences, University of Zürich, Zürich, Switzerland

² Solid Tumour and Biomarkers Programme, Centre for Applied Medical Research and Department of Histology and Pathology, University of Navarra, Pamplona, Spain

*Correspondence to: B Bodenmiller, Institute of Molecular Life Sciences, University of Zürich, Winterthurerstrasse 190, Y11-J-82, 8057, Zürich, Switzerland. E-mail: bernd.bodenmiller@imls.uzh.ch

Abstract

Imaging mass cytometry is a novel imaging modality that enables simultaneous antibody-based detection of >40 epitopes and molecules in tissue sections at subcellular resolution by the use of isotopically pure metal tags. Essential for any imaging approach in which antigen detection is performed is counterstaining, which reveals the overall structure of the tissue. Counterstaining is necessary because antigens of interest are often present in only a small subset of cells, and the rest of the tissue structures are not visible. As most biological tissues are nearly transparent or non-fluorescent, chromogenic reagents such as haematoxylin (for immunohistochemistry) or fluorescent dyes such as 4',6-diamidino-2-phenylindole (which stains nuclei for epifluorescence and confocal microscopy) are utilized. Here, we describe a metal-based counterstain for imaging mass cytometry based on simple oxidation and subsequent covalent binding of the tissue components to ruthenium tetroxide (RuO_4). RuO_4 counterstaining reveals general tissue structure both in areas with high cell content and in stromal areas with low cellularity and fibrous or hyaline material in a manner analogous to haematoxylin in immunohistochemical counterstaining or eosin or other anionic dyes in conventional histology. Our new counterstain approach is applicable to any metal-based imaging technique, and will facilitate the adaptation of imaging mass cytometry for routine applications in clinical and research laboratories.

Copyright © 2018 Pathological Society of Great Britain and Ireland. Published by John Wiley & Sons, Ltd.

Keywords: imaging mass cytometry; IMC; metal counterstaining; ruthenium tetroxide; high-throughput histology; next-generation immunohistochemistry

Received 18 November 2017; Revised 9 January 2018; Accepted 30 January 2018

No conflicts of interest were declared.

Introduction

Most biological tissues are nearly transparent and display no inherent colour [1,2] or fluorescent properties [3] that reveal overall tissue structure. A plethora of techniques have been developed over the past several decades to provide contrast to tissue components [1,3,4]. Many of these methods are general staining procedures, often referred to as counterstaining, that involve plant-derived stains such as haematoxylin or safranin, or chemical dyes such as eosin, fuchsin, methylene blue, toluidine blue, and methyl green [5,6]. These compounds stain tissues because of the chemical characteristics of the target molecules. For example, basic colorants such as haematoxylin stain acidic DNA, and the acidic colorant eosin binds to ionized cationic groups of the side chains of lysine or arginine, which are two amino acids that are present in most proteins [7]. Other colorants show specificity for certain tissue components. This is the case for aniline blue, which avidly binds collagen [8], and for 4',6-diamidino-2-phenylindole (DAPI), which binds to

DNA and is used to reveal nuclei [9]. These general staining reagents complement more specific molecular methods such as *in situ* hybridization, which is used to detect specific RNA transcripts, and immunohistochemistry or immunofluorescence, which are used to detect antibody-based reactions. Heavy metal-containing chemicals such as osmium tetroxide (OsO_4) platinum blue, uranyl acetate, and lead citrate are also used as counterstains for electron microscopy [10].

Our laboratory recently developed a new modality of histological staining: imaging mass cytometry (IMC) [11,12]. By the use of isotopically pure rare earth metals bound to antibodies, it is possible to detect >40 antigens simultaneously in the same tissue section with a time-of-flight mass spectrometer coupled to a laser ablation device that raster-scans the tissue (normally performed at $1 \mu\text{m}^2$ per laser ablation pulse), though it is possible to raster-scan at submicrometre resolution (e.g. $0.25 \mu\text{m}^2$ per ablation pulse) at the expense of lower sensitivity and acquisition speed. Despite the fact that this technology functions very differently from classic microscopy techniques, it is truly a microscopy modality, with similar resolution and antigen–antibody

reaction immunohistochemistry-like-based imaging. This means that, in order to have a general view of the studied structure, a counterstaining method to observe the tissue is required. In IMC, only atoms with an atomic mass of >80 Da are detected, making most of the available counterstaining reagents for light or fluorescence microscopy useless for IMC. To overcome this limitation, we have developed a simple, rapid counterstaining method based on incubation of tissue in ruthenium tetroxide (RuO_4) solution. RuO_4 staining readily reveals the tissue architecture, and does not interfere with antibody binding.

Materials and methods

Specimens

For this study, archived formalin-fixed paraffin-embedded specimens of patients diagnosed with non-small-cell lung carcinoma (NSCLC) who underwent surgery at the Clínica Universidad de Navarra (Pamplona, Spain) between 2000 and 2017 were selected. The inclusion criteria were: complete resection of the primary lung tumour, absence of cancer within the 5 years prior to lung cancer surgery, absence of neoadjuvant therapy before surgery, and available clinicopathological information. A tissue microarray (TMA) containing representative areas of 150 NSCLC specimens was constructed with a manual tissue arrayer (MTA-1; Beecher Instruments, Sun prairie, WI, USA). After histological examination of the NSCLC specimens, the TMAs were constructed from triplicate 1-mm tissue cores from each tumour. The study protocol was approved by the institutional ethical committee. Written informed consent was obtained from each patient. The cohort of samples is deposited in our programme institutional collection registered in the Spanish National Biobank Register (C.0000960). For the present study, some representative samples of this TMA were analysed. One representative sample from the cohort is shown in the main figures. Other samples are utilized in the supplementary figures.

Tissue preparation

Tissues were fixed with 3.7% phosphate-buffered formalin, dehydrated, paraffin-embedded, and sectioned to a thickness of 5 μm with a microtome. Tissue slides were heated at 60 °C for 30 min to melt the paraffin, which was then removed by submerging the slides in xylene. Tissues were then hydrated with a series of ethanol/water mixtures. Hydrated tissues were placed in Coplin jars containing Tris–HCl buffer for antigen retrieval. Tissues were heated for 40 min at 95 °C in the antigen retrieval solution in a pressure cooker. After antigen retrieval, slides were washed with phosphate-buffered saline (PBS). Slides were then blocked with 1% serum and 1% human Fc-Block (Miltenyi Biotech, San Diego, CA, USA) in PBS for 30 min at room temperature.

Antibody staining

A mixture of 29 metal-conjugated antibodies (supplementary material, Table S1), labelled by the use of Max-Par labelling kits (Fluidigm, South San Francisco, CA, USA), were added, and slides were incubated overnight at 4 °C in a wet chamber. After antibody incubation, slides were washed twice with PBS for 10 min. It is important that the buffer used in this wash step does not contain protein.

Counterstaining

An electron microscopy-grade stock solution of 0.5% RuO_4 , buffered in PBS, was obtained from Electron Microscopy Sciences (Hatfield, PA, USA). Slides were incubated with a freshly prepared 0.0005% w/v solution of RuO_4 prepared by dilution of the 0.5% stock solution in PBS. RuO_4 is chemically similar to OsO_4 , which is used in the processing of specimens for electron microscopy. RuO_4 was chosen because it is less toxic than OsO_4 (Level 1 health hazard for RuO_4 [13] versus level 4 for OsO_4 [14] standard working solutions, respectively). However, it evaporates rapidly; therefore, it is important to work under a fume hood, keep solutions on ice, work rapidly, and dispose of the residues appropriately. Standard procedures applied in any electron microscopy laboratory are appropriate for handling this chemical. The RuO_4 solution was added to the slides. The slides were incubated for 3 min, placed in distilled water for 10 s to remove salt, and quickly air-dried.

Image acquisition

Images were acquired with a Fluidigm Hyperion Laser Scanning Module coupled to a Helios Mass Cytometer, with the following settings: 3-dB laser attenuation, 0.23 l/min helium gas flow, and 0.8 l/min argon flow. Results in .mcd and .txt files containing the acquired data were generated by Fluidigm's CyTOF software v6.7.1014.

For image processing, we used histoCAT++ and IMCReader OSX Viewer software v2.2 (<http://www.bodenmillerlab.org/research-2/histocal-2/>). histoCAT++ is a new software application that we introduce here. Built on histoCAT, the platform recently published by us [15], histoCAT++ features advanced visualization options, import/export functions for IMC data (.mcd and .txt files), and other imaging formats (.tiff, .jpg, etc). histoCAT++ is written in the C and Objective-C programming languages. All images in this article were prepared with histoCAT++, including the pseudo-haematoxylin/eosin and pseudo-IHC images.

Results

Lung cancer tissue samples were stained with a panel of 29 metal-tagged antibodies (supplementary material, Table S1 and Figure S2). Examples of tissue stained with antibodies that stained very few cells (CD68, vimentin, and CD45) are shown in Figure 1B,D,F,H.

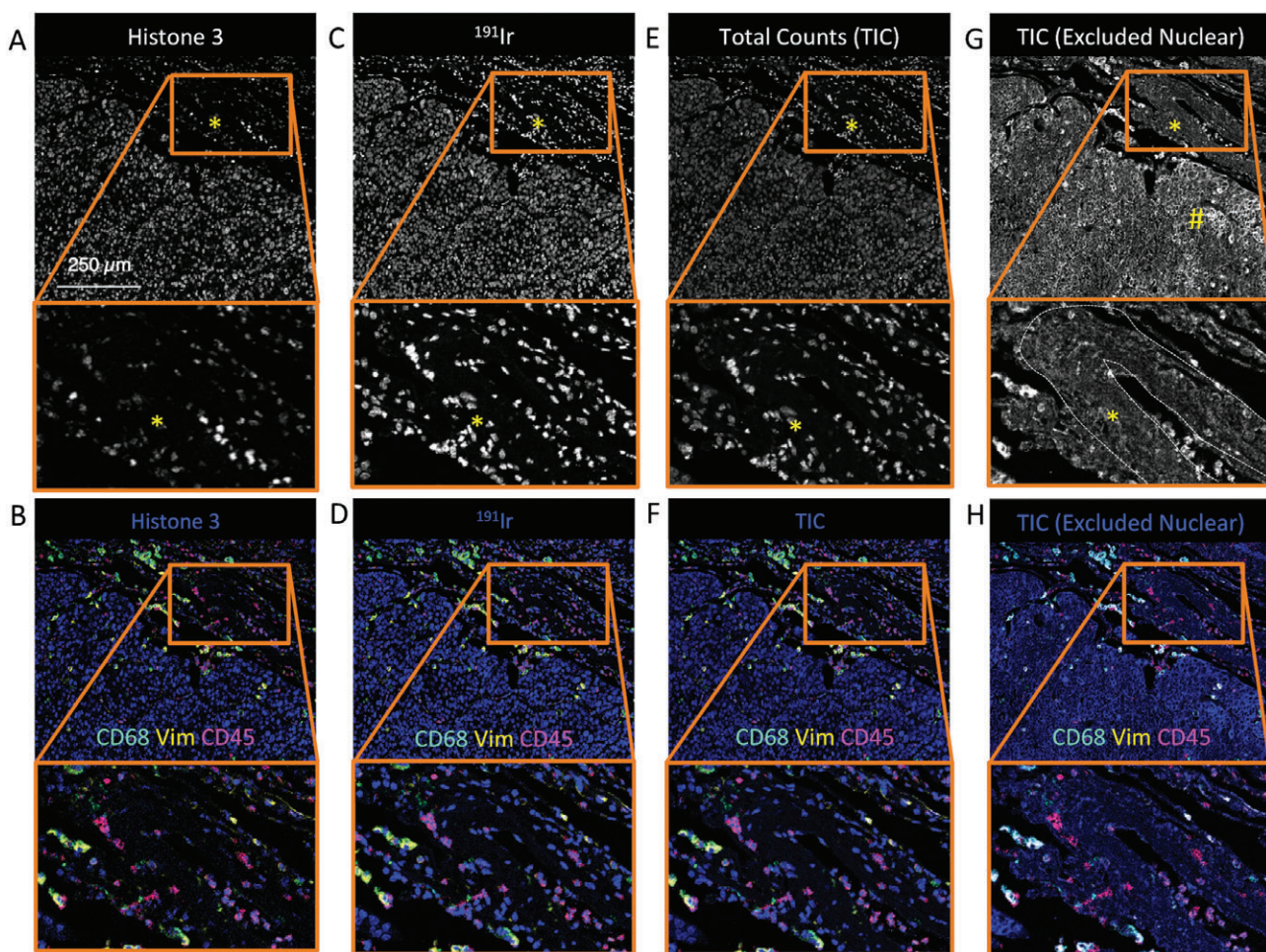


Figure 1. IMC analysis of a representative lung cancer formalin-fixed paraffin-embedded sample tissue section counterstained with (A) antibody against histone-3 conjugated to ^{113}In , (B) histone-3 signal as counterstain for CD68, vimentin, and CD45, (C) ^{191}Ir revealing DNA, (D) ^{191}Ir as counterstain for CD68, vimentin, and CD45, (E) TIC signal from all of the metals in the utilized panel, (F) TIC as counterstain for CD68, vimentin, and CD45, (G) TIC from all metals in the utilized panel, excluding nuclear signals (^{191}Ir , ^{193}Ir , and ^{113}In -histone-3), and (H) TIC, excluding nuclear signals, as counterstain for CD68, vimentin, and CD45.

Even considered together, cells expressing these antigens occupied a fraction of the imaged area, so a counterstain is necessary to reveal tissue structure.

As counterstains, we first tested two nuclear stains: a metal-tagged anti-histone-3 antibody and iridium, which binds to double-stranded DNA (Figure 1A–D). Both of these reagents allowed the detection of most, if not all, nuclei present in the imaged area. The nuclear stains resulted in a counterstaining pattern similar to that of DAPI or TOPRO-3, which are used for fluorescence microscopy [3]. Second, we tested ‘all metal signals’, or total ion counts (TICs), from all metal-labelled antibodies in the panel, either including the nuclear markers, which dominate the overall output channel, or excluding them, as proposed by Chang *et al* [16] (Figure 1E–H). The TIC excluding the nuclear signal better revealed the tissue structure than did either anti-histone-3 or iridium staining. With the TIC excluding the nuclear markers, certain acellular areas, such as the elastic stroma around an arterial blood vessel, were visible; these were not visible when only a nuclear counterstain was used (Figure 1A,C,E,G, asterisks; insets show a detail of the arterial vessel area, and the wall is marked by dotted

lines). None of the strategies relying on TIC uniformly stains tissue structures. For example, the signal was significantly higher in the tumour region (Figure 1G, marked with #) than in the stroma when TIC with exclusion of nuclear markers was used. To observe the areas with low signal, the contrast must be adjusted, and this may lead to saturation of higher total count areas, making this method non-optimal.

To achieve a more uniform metal-based counterstaining approach for IMC, we used RuO_4 , which reacts with carbon–carbon double bonds. Importantly, Ru can be detected in the mass range of 96–104, which does not overlap with the range of the metal isotopes used for antibody labelling. Staining of lung cancer tissue with RuO_4 resulted in similar intensities of counterstaining of all tissue components (Figure 2A). Thus, RuO_4 counterstaining did not mask signals from antigens expressed on very few cells (Figure 2B). In combination with iridium, RuO_4 counterstaining can be used to mimic the classic histological staining for bright-field haematoxylin and eosin (H&E) when channels are pseudocoloured in purple and fuchsia, respectively, over a white background (Figure 2C). We call this

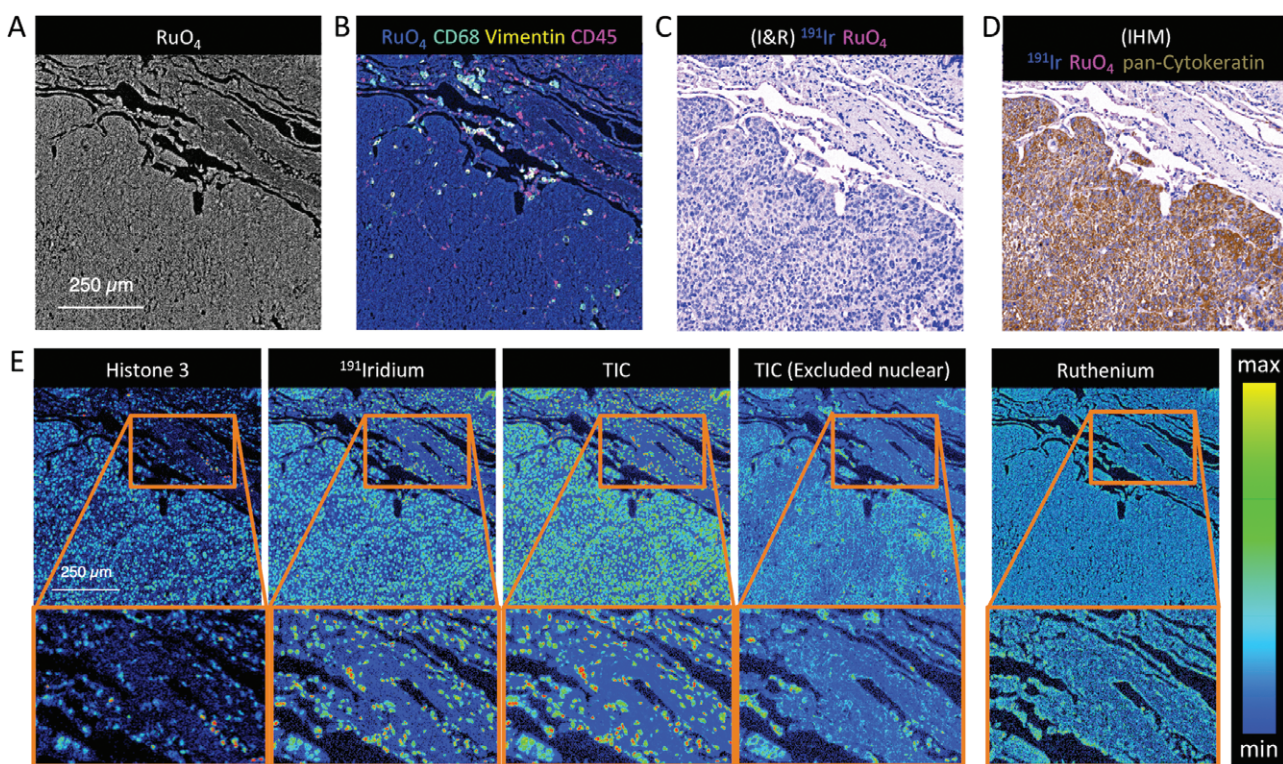


Figure 2. IMC analysis of the same tissue as in Figure 1 stained with RuO₄ as a counterstain. (A) Signal from all ruthenium isotopes. (B) Ruthenium as counterstain for CD68, vimentin, and CD45. (C) Pseudocoloured nuclear (¹⁹¹Ir) and tissue-wide RuO₄ staining mimicking H&E staining. (D) Pseudocoloured immunohistochemistry signal from ¹⁷⁵Lu-pan-cytokeratin antibody in a sample counterstained with ¹⁹¹Ir and RuO₄ mimicking diaminobenzidine–HRP immunohistochemistry counterstained with H&E. (E) Comparison of IMC counterstaining methods using a colour-based scale. TIC indicates summed total ion counts.

strategy I&R (for iridium and ruthenium), by analogy with the term H&E. Furthermore, by pseudocolouring additional antibody-based markers in brown, images can be generated that are akin to those generated by staining samples using diaminobenzidine-horseradish peroxidase (HRP)-based immunohistochemistry subsequently counterstained with haematoxylin and/or eosin (Figure 2D).

RuO₄ counterstaining resulted in a more homogeneous pattern throughout the tissue than the other counterstaining methods evaluated (Figure 2E). Importantly, RuO₄ counterstaining did not interfere with the detection of signals due to metal-tagged antibodies (supplementary material, Figures S1 and S2, and Table S2). None of the proteins analysed that were detected in the tissue showed a noticeable decrease in antibody signal due to RuO₄ treatment. Importantly, this observation applied both to antibodies detected with high intensity, such as α-smooth muscle actin, and to those showing specific signals just over the background, as in the case of CD20, CD45, and pan-keratin (supplementary material, Figures S1 and S2, and Table S2).

Discussion

In imaging and microscopy techniques, counterstains are used to reveal the general tissue structure, identify the objects of interest, and correctly find the focal point.

Some counterstaining methods rely on reagents that bind a wide range of structures non-specifically, achieving a general contrast for all organic components of the tissue; this is the case for methylene blue staining. The second approach is to utilize stains that bind components that are expected to be very abundant in the tissue, such as DNA or collagen. Examples of these reagents are DAPI, Hoechst, TOPRO, and DRAQ, which are DNA-binding fluorophores that efficiently stain nuclei [3]. Haematoxylin is another general stain used in light microscopy that reveals nuclei and other structures such as acid granules in leukocytes.

We sought to develop a method to counterstain tissues for IMC. RuO₄ has been used in electron microscopy to add contrast to lipid bilayers, as RuO₄ covalently reacts with fatty acid chain carbon–carbon double bonds, making them more electron-dense. Membranes become brittle during processing, and RuO₄-mediated crosslinking helps to preserve the bilayer structure, making it visible in the electron microscope. In IMC, most lipids are significantly removed by alcohols during tissue processing for paraffin embedding. When RuO₄ is applied to tissues stained with antibodies, RuO₄ rapidly and irreversibly reacts with non-lipid molecules containing carbon–carbon double bonds, including proteins. All ruthenium isotopes have atomic masses of >80 Da (from 96 to 104 Da), which are within the mass range of the mass spectrometer. Ruthenium isotopes do not interfere with signals from the lanthanide series isotopes, which

are the isotopes normally used to label antibodies for IMC. Importantly, we have shown here that RuO₄ applied after antibody staining does not interfere with the quantification of antibody-based staining, and might even crosslink the metal-labelled antibodies to cells, preserving antibody signals [17]. These properties make RuO₄ an ideal counterstain for IMC. OsO₄ is also widely used in electron microscopy, has similar properties, and could, in theory, also be used as a counterstain for IMC; however, it is considerably more toxic than RuO₄ [13,14].

RuO₄ binds to all tissue structures with similar affinity, thus producing images with flat profiles that do not need intensity readjustment. This approach is therefore advantageous as compared with other solutions to the mass cytometry counterstain problem, such as the one proposed by Chang *et al* [16], in which intensities of all channels are summed to produce a composite counterstain channel. When channel intensities are summed, dominant channels obscure the contributions of channels with low signals. As shown here, the nuclear stains iridium and histone-3 dominate other signals, producing a counterstain composite channel similar to that of the nuclear stain, and artificial saturation of the signal is needed to reveal structures such as the stromal collagen fibres. Furthermore, with the composite channel approach, some structures may not be detected by any of the antibodies used in the experiment. Also, the total counts depend on the antibodies used in the staining panel, so results are not comparable unless the antibody panels are identical. Finally, an additional advantage of a simple, tissue-wide counterstain such as RuO₄ is that, potentially, changes in tissue thickness could be detected. By normalizing for tissue thickness based on RuO₄ intensity, more accurate quantification of the signal for the antibodies utilized can be achieved [18].

We also found that RuO₄ in combination with a nuclear marker, such as histone-3, can be used to mimic H&E or immunohistochemistry when images are pseudocoloured; we call these strategies I&R and pseudo-IHM (for iridium and ruthenium, and immuno-histo-metal detection, respectively). These strategies will enable comparison of results from mass cytometry-based technologies with classic histological methods by pathologists, who are mainly trained with H&E stained tissues, as well as by existing computer vision and machine learning-based algorithms, which have been developed using large sets of H&E images. We expect that use of RuO₄ for counterstaining in tissue imaging will expand the use of IMC and multiplexed ion beam imaging techniques, and will make comparison of data collected by different laboratories or at different times feasible. To contribute to this, we introduce histoCAT++, an extension of our IMC image analysis toolbox histoCAT [15]. histoCAT++ enables efficient and easy image processing and image generation from IMC data, generating images akin to those obtained with classic histological techniques, I&R and IHM

being analogous to H&E and immunohistochemistry, respectively.

Acknowledgements

We would like to thank Stefanie Engler and Andrea Jacobs for technical support. This work was supported by the Swiss National Science Foundation (SNSF) R'Equip grant 316030-139220, an SNSF Assistant Professorship grant PP00P3-144874, the PhosphenetPPM and MetastasiX SystemsX grants, and funding from the European Research Council (ERC) under the European Union's Seventh Framework Programme (FP/2007-2013)/ERC Grant Agreement no. 336921. LMM was partially funded by grants from the Spanish Ministry of Economy and Innovation-FEDER ISCIII: FIS (PI16/01821), and from the AECC Scientific Foundation (GCB14-2170).

Author contributions statement

RC performed the experiments, analysed data, and wrote the histoCAT++ software. RC and BB conceived and designed the method. LMM coordinated clinical sample acquisition and ethics approval. RC and BB wrote the manuscript. All authors edited the manuscript.

References

- Alturkistani HA, Tashkandi FM, Mohammedsaleh ZM. Histological stains: a literature review and case study. *Glob J Health Sci* 2015; **8**: 72–79.
- Mandhan P, Qi BQ, Keenan JI, *et al*. Counterstaining improves visualization of the myenteric plexus in immunolabelled whole-mount preparations. *J Fluoresc* 2006; **16**: 655–668.
- Schmued LC, Swanson LW, Sawchenko PE. Some fluorescent counterstains for neuroanatomical studies. *J Histochem Cytochem* 1982; **30**: 123–128.
- Bink K, Walch A, Feuchtinger A, *et al*. TO-PRO-3 is an optimal fluorescent dye for nuclear counterstaining in dual-colour FISH on paraffin sections. *Histochem Cell Biol* 2001; **115**: 293–239.
- Kather JN, Weis CA, Marx A, *et al*. New colors for histology: optimized bivariate color maps increase perceptual contrast in histological images. *PLoS One* 2015; **10**: e0145572.
- Guidry G. A method for counterstaining tissues in conjunction with the glyoxylic acid condensation reaction for detection of biogenic amines. *J Histochem Cytochem* 1999; **47**: 261–264.
- Fischer AH, Jacobson KA, Rose J, *et al*. Hematoxylin and eosin staining of tissue and cell sections. *CSH Protoc* 2008.
- Lillie RD, Tracy RE, Pizzolato P, *et al*. Differential staining of collagen types in paraffin sections: a color change in degraded forms. *Virchows Arch A Pathol Anat Histol* 1980; **386**: 153–159.
- James TW, Jope C. Visualization by fluorescence of chloroplast DNA in higher plants by means of the DNA-specific probe 4'6-diamidino-2-phenylindole. *J Cell Biol* 1978; **79**: 623–630.
- Inaga S, Katsumoto T, Tanaka K, *et al*. Platinum blue as an alternative to uranyl acetate for staining in transmission electron microscopy. *Arch Histol Cytol* 2007; **70**: 43–49.
- Giesen C, Wang HA, Schapiro D, *et al*. Highly multiplexed imaging of tumor tissues with subcellular resolution by mass cytometry. *Nat Methods* 2014; **11**: 417–422.

12. Bodenmiller B. Multiplexed epitope-based tissue imaging for discovery and healthcare applications. *Cell Syst* 2016; **2**: 225–238.
13. Ruthenium Tetroxide MSDS. [Accessed 18 November 2017]. Available from: <https://www.emsdiasum.com/microscopy/technical/msds/20700-05.pdf>
14. Osmium Tetroxide MSDS. [Accessed 18 November 2017]. Available from: <https://www.emsdiasum.com/microscopy/technical/msds/19100.pdf>
15. Schapiro D, Jackson HW, Raghuraman S, et al. histoCAT: analysis of cell phenotypes and interactions in multiplex image cytometry data. *Nat Methods* 2017; **14**: 873–876.
16. Chang Q, Ornatsky OI, Siddiqui I, et al. Biodistribution of cisplatin revealed by imaging mass cytometry identifies extensive collagen binding in tumor and normal tissues. *Sci Rep* 2016; **6**: 36641.
17. Carpenter DC, Nebel BR. Ruthenium tetroxide as a fixative in cytology. *Science* 1931; **74**: 154–155.
18. Frick DA, Giesen C, Hemmerle T, et al. An internal standardization strategy for quantitative immunoassay tissue imaging using laser ablation inductively coupled plasma mass spectrometry. *J Anal At Spectrom* 2015; **30**: 254–259.

SUPPLEMENTARY MATERIAL ONLINE

Supplementary figure legends

Figure S1. Imaging Mass Cytometry signal comparison with or without ruthenium tetroxide (RuO_4) as counterstain

Figure S2. Imaging Mass Cytometry signal comparison with or without ruthenium tetroxide (RuO_4) as counterstain for all antibodies used in the panel in a lung cancer sample expressing most markers

Table S1. Antibodies used in the staining panel

Table S2. Signal counts for all antibodies with or without RuO_4 counterstaining shown in supplementary materials, Figure S2

75 Years ago in the *Journal of Pathology...*

The complement activity of the serum of healthy persons, mothers and new-born infants

B. Traub

The action of chemotherapeutic drugs (including proflavine) and excipients on healthy tissue

F. R. Selbie and James McIntosh

A rapid silver stain for nerve fibres in formol-fixed paraffin sections of the human spinal cord and medulla

J. F. A. McManus

To view these articles, and more, please visit:

www.thejournalofpathology.com

Click 'ALL ISSUES (1892 - 2018)', to read articles going right back to Volume 1, Issue 1.

The Journal of Pathology
Understanding Disease

